Supplementary information

Endothelial O-glycan deficiency causes blood/lymphatic misconnections and consequent fatty liver disease in mice

Jianxin Fu,[1] Holger Gerhardt,[2] J. Michael McDaniel,[1] Baoyun Xia,[3] Xiaowei Liu,[1] Lacramioara Ivanciu,[1] Annelii Ny,[4] Karlien Hermans,[4] Robert Silasi-Mansat,[1] Samuel McGee,[1] Emma Nye[2], Tongzhong Ju,[3] Maria I. Ramirez,[5] Peter Carmeliet,[4] Richard D. Cummings,[3] Florea Lupu,[1] and Lijun Xia[1,6]

[1]Cardiovascular Biology Research Program, Oklahoma Medical Research Foundation, Oklahoma City, Oklahoma, USA. [2]Vascular Biology Laboratory, Cancer Research UK London Research Institute, London, United Kingdom. [3]Department of Biochemistry, Emory University School of Medicine, Atlanta, Georgia, USA. [4]The Center for Transgene Technology and Gene Therapy, Katholieke Universiteit Leuven, Leuven, Belgium. [5]Department of Medicine, Boston University School of Medicine, Boston, Massachusetts, USA. [6]Department of Biochemistry and Molecular Biology and Oklahoma Center for Medical Glycobiology, University of Oklahoma Health Sciences Center, Oklahoma City, Oklahoma, USA

The authors have declared that no conflict of interest exists.

Nonstandard abbreviations: MS, mass spectrometry; HPA, *Helix pomatia* agglutinin; Prox1, Prospero-related homeobox 1

Address correspondence to: Lijun Xia, Cardiovascular Biology Research Program, Oklahoma Medical Research Foundation, 825 N.E. 13th Street, Oklahoma City, Oklahoma 73104, USA. Phone: (405) 271-7892; Fax: (405) 271-3137; e-mail: lijun-xia@omrf.org.

Supplementary methods

Mice. To generate bone marrow-transplanted chimeric mice, six-week-old recipient wild-type B6.SJL mice (CD45.1, The Jackson Laboratory) or EHC T-syn$^{-/-}$ mice (CD45.2) were lethally irradiated (2 doses of 6.5 Gy each, 3 h apart) using a ^{137}Cs source and injected intravenously with unfractionated bone marrow cells (1×10^7 per mouse in 200 µl saline) from femora of the respective donors. Six weeks after transplantation, engraftment was assessed by flow cytometric analysis of peripheral blood. After red blood cell lysis, the leukocytes were stained with FITC-labeled anti–mouse CD45.1 mAb (clone A20, BD Biosciences) and phycoerythrin-conjugated anti–mouse CD45.2 mAb (clone 104, BD Biosciences) and analyzed on a FACSCalibur (BD Biosciences). Data were collected and analyzed using the CellQuest Pro (BD Biosciences). Recipient mice were kept for up to 9 months for analysis.

Microscopy. For lectin angiography of hindbrain, embryos (E11.5) were fixed in 4% PFA in PBS at 4°C over night. Hindbrains were dissected clean from surrounding tissue and subjected to whole-mount staining with biotinylated isolectin B4 *Griffonia simplicifolia* (20 µg/ml; Sigma-Aldrich). 3D analysis was performed on a Zeiss LSM 510 Meta confocal laser-scanning microscope using original Zeiss software (1).

For fluorescence immunostaining of endothelial cells, primary skin endothelial cells were cultured on glass coverslips for 4 h. After brief wash, cells were blocked with 5% BSA and 5% normal donkey serum in PBS for 1 h on ice and incubated with rat anti-mouse podoplanin mAb (clone 8F11, 10 µg/ml; MBL) in 1%BSA/PBS for 1 h on ice. Next, the specimens were washed and fixed with 4% PFA for 10 min at room

temperature. After wash, the cells were incubated with rabbit anti-Prox-1 (10 μg/ml) overnight at 4^{o}C. Samples were incubated with FITC-conjugated donkey anti-rat IgG (10 μg/ml) and Cy3-conjugated donkey anti-rabbit IgG (10 μg/ml) for 1 h at room temperature and then examined with a Nikon C1 confocal microscope.

Semi-quantitative RT-PCR. Total RNA was prepared from endothelial cells with TRIzol reagent (Invitrogen) treated with DNase I (Ambion). cDNA was synthesized from 2 μg total RNA using M-MLV reverse transcriptase (Invitrogen) and oligo dT primer. PCR amplification was carried out with GeneAmp equipment (PCR system 2400; Perkin-Elmer). The quantity of RNA was confirmed by agarose gel electrophoresis with reference to the internal control, GAPDH.

Morpholino knockdown in Xenopus laevis. Fertilized *Xenopus* eggs were achieved from WT female frogs (Nasco Biology), after natural fertilizations with *Tg(Flk1:eGFP)* transgenic males generated in house (manuscript in preparation).

Eggs were injected with 25 to 100 ng morpholino (Gene Tools) into the one cell stage as described (2). The ATG-targeted antisense morpholino 5' – CCTTGGCACATATAATTGACATTGC – 3' were designed based on sequences achieved when cloning the gene from cDNA generated from the Nasco Biology strain. This sequence was found to be identical to the published GenBank *Xenopus laevis* sequences of xT-syn (BC073496). As control a standard control morpholino provided by Gene Tools was used 5'–CCTCTTACCTCAGTTACAATTTATA–3'.

The efficacy of the morpholino was confirmed by using cloning a chimeric xT-

syn/luciferase fusion reporter construct and evaluating it in the reticulocyte assay (2). Briefly, a reporter plasmid (pGL4-T7-xT-syn-Luc2) was constructed. The plasmid contained, from 5' to 3', the T7 promotor, a short sequence of the *Xenopus* T-syn sequence (40 nct upstream and 40 nct downstream of the ATG), the luciferase open reading frame and a SV40 poly-adenylation signal. Translation of pGL4-T7-xTsyn-Luc2, using the reticulocyte lysate assay, resulted in the production of a chimeric protein, containing 13 amino acid residues of *Xenopus* T-syn and an intact full length luciferase, the activity of which was used as a measure of the translation efficiency. Injected embryos were staged according to Nieuwkoop and Faber (3) and grown at 18°C until gastrulation was completed and subsequently at 22°C. Live screening of general development, heart beating, blood flow, lymph heart (LH) beating, and the presence or absence of blood spots and edema at stage 48 (8 dpf) using a Zeiss SV11 stereomicroscope. To visualize the vasculature in the trunk of *Tg(Flk1:eGFP)* transgenic embryos, tadpoles were briefly anaesthetized (0.02% of 3-aminobenzoic acid ethyl ester) and the eGFP positive blood-and lymphatic vessels were documented with a Zeiss SteREO Lumar V.12 stereomicroscope equipped with an AxioCam MrC5 (Zeiss) digital camera and controlled with the AxioVision 4.4 software (Zeiss).

Morpholino knockdown in zebrafish. Tg(fli1:EGFP)^{y1} (4) and *Tg(gata-1:DsRed*) (5) zebrafish were maintained under standard laboratory conditions. Embryos were kept in 0.3x Danieau/PTU (embryo water) at 28°C. The following gene-specific antisense morpolino oligonucleotides were purchased from Gene Tools (LLC): 5'-GTATGTAGAGACCCTCACCTCACAG -3' (zTsyn-MO-ATG), 5'-

TTTCTGCCACGTTATTACCTGTATG -3' (zTsyn-MO-Splice), targeting the translation initiation site and the boundary between the first exon and the first intron of zebrafish *T-syn* (GenBank number NM_200051.1), respectively.

The silencing efficiency of zTsyn-MO-ATG was determined as previously described using a luciferase reporter assay (2). Briefly, a zTsyn specific 5' UTR fragment of approximately 85 nucleotides, containing the zTsyn start codon and the target sequence of zTsyn-MO-ATG, was cloned upstream and in frame of an open reading frame of the luciferase reporter gene (lacking the start codon). Expression of this chimeric reporter protein in the erythrocyte lysate assay was monitored via luminometry. The efficiencies of the splice site-directed morpholino was directed by PCR using the following primers spanning the first intron-exon boundary: 5' – AGGAGAGGTCGGCTCTTTTC – 3' (forward primer) and 5' – CTGGAGTCTCCTGCCTTGAC – 3' (reverse primer).

Different doses of morpholinos were injected into single- to four-cell stage embryos, using procedures as previously described (6) and embryos were further incubated in embryo water at 28°C until 2, 3 and 7 days post fertilization (dpf). At these time points, between 30 and 60 injected embryos per experiment were analyzed and each experiment was repeated at least two times. All data shown here were obtained after injection of 18 ng of morpholino. Control embryos were injected with injection buffer (0.1% phenol red, 0.4M KCl). Confocal imaging of embryos was performed using a Zeiss laser scanning microscope LSM510 and the 488 nm laser emission was supplied by an argon laser.

Supplementary Results

Characterization of T-synthase in zebrafish and Xenopus laevis.

Xenopus laevis

A morpholino targeting the translation initiation site of *Xenopus* laevis T-syn (xT-syn) was used to lower protein levels in *Xenopus laevis* embryos. The efficacy of the morpholino was demonstrated in the reticulocyte assay, where it dose dependently inhibited translation of a chimeric xT-syn/luciferase fusion reporter construct (Supplemental Figure 6A) (2).

The xT-syn morpholino was injected in 1-cell stage embryos in the *Tg(Flk1:eGFP)* transgenic stain, expressing GFP under the xVEGFR-2 promoter in blood and lymphatic vasculature (complete description of this transgenic line will be reported elsewhere). Morpholinos were injected at doses ranging from 25 ng to 100 ng. At all doses of morpholino, xT-syn knockdown ($xTsyn^{KD}$) embryos exhibited a normal morphology with no apparent signs of hemorrhaging, indistinguishable from control-injected tadpoles (Supplemental Figure 6B, left panel bright field images). In addition, fluorescent microscopy revealed that both blood- and lymph vessels in the $xT\text{-}syn^{KD}$ embryos formed correctly and had normal appearance as compared to the controls; lymph vessels also separated normally from blood vessels (Supplemental Figure 6B, left panel fluorescent images, higher magnifications in right panels).

Zebrafish

To knockdown protein levels of T-syn in zebrafish (zT-syn), we injected in one-cell stage embryos two different zT-syn-specific antisense morpholino oligonucleotides, zTsyn-MO-ATG and zTsyn-MO-Splice, targeting the translational start site or the boundary between the first exon and the first intron of zT-syn, respectively. zTsyn-MO-ATG dose-

dependently inhibited translation of a chimeric mRNA transcript, consisting of a short 5'UTR and ATG of the target mRNA, fused to the remainder of the luciferase open reading frame (2) (Supplemental Figure 7A), whereas zTsyn-MO-Splice dose-dependently blocked normal splicing of the first intron as evidenced by RT-PCR amplification of zT-syn-specific sequences, spanning the first intron boundary, using cDNA from zTsyn-MO-Splice-injected embryos of 2 dpf (Supplemental Figure 7B).

Macroscopic inspection of zT-syn knockdown ($zTsyn^{KD}$) embryos using either morpholino revealed that they had a normal body shape and developmental growth rate. Also, blood flow in axial vessels and intersomitic vessels (ISVs) appeared normal and no sites of hemorrhage were observed during the entire duration of analysis (until 6 dpf) (Supplemental Figure 7C).

To visualize (lymph) vascular defects in detail, we analyzed *Tg(Fli1:EGFP)*^{y1} zebrafish embryos expressing GFP in both blood and lymph vessels (4) between 1 and 6 dpf with confocal microscopy (Supplemental Figure 7D). Even at the highest dose of morpholino (18 ng per embryo), both the axial vessels (dorsal aorta and posterior cardinal vein) and the ISVs developed normally in $zTsyn^{KD}$ embryos. By 3 dpf, the parachordal vessel (PAV), from which the lymphatic endothelial cells originate (7), developed normally and appeared morphologically indistinguishable from the PAV in control embryos. Finally, at 6 dpf, the lymphatic thoracic duct also developed normally over its entire length in the trunk of $zTsyn^{KD}$ embryos.

To further evaluate whether any aberrant blood and lymph vascular connections might result in a blood filled thoracic duct in $zTsyn^{KD}$ embryos, we also analyzed *Tg(gata-1:DsRed)* embryos, expressing DsRed in their erythrocytes (5) (Supplemental

Figure 7D, right panels). Similar to control embryos, zTsyn^{KD} embryos had a regular blood flow in their trunk vasculature, including in the dorsal aorta, posterior cardinal vein and the ISVs from 2 dpf onward; however, erythrocytes were never observed in the thoracic duct in 6 dpf zTsyn^{KD} embryos, indicating that blood and lymph vessels segregated normally. This finding was also confirmed in *Tg(Fli1:EGFP)^{y1}* embryos subjected to angiography at 6 dpf (Supplemental Figure 7E). Following heart injection of dextran tetramethylrhodamin the major blood vessels, including the dorsal aorta, posterior cardinal vein and ISVs were labeled, however no dye was ever observed in the thoracic duct of both control and zTsyn^{KD} embryos. All together, our data suggest that there are no obvious defects, nor aberrant connections between blood and lymph vessel in zTsynKD embryos.

References

1. Gerhardt, H., Ruhrberg, C., Abramsson, A., Fujisawa, H., Shima, D., and Betsholtz, C. 2004. Neuropilin-1 is required for endothelial tip cell guidance in the developing central nervous system. *Dev. Dyn.* 231:503-509.
2. Ny, A., Koch, M., Schneider, M., Neven, E., Tong, R.T., Maity, S., Fischer, C., Plaisance, S., Lambrechts, D., Heligon, C., et al. 2005. A genetic Xenopus laevis tadpole model to study lymphangiogenesis. *Nat. Med.* 11:998-1004.
3. Nieuwkoop, P.J.F., J. . 1994. *Normal table of Xenopus Laevis (Daudin): A systematical and chronological survey of the development from the fertilized egg till the end of metamorphosis*. New York: Garand Publishing Inc.
4. Lawson, N.D., and Weinstein, B.M. 2002. In vivo imaging of embryonic vascular development using transgenic zebrafish. *Dev. Biol.* 248:307-318.
5. Traver, D., Paw, B.H., Poss, K.D., Penberthy, W.T., Lin, S., and Zon, L.I. 2003. Transplantation and in vivo imaging of multilineage engraftment in zebrafish bloodless mutants. *Nat. Immunol.* 4:1238-1246.
6. Stalmans, I., Ng, Y.S., Rohan, R., Fruttiger, M., Bouche, A., Yuce, A., Fujisawa, H., Hermans, B., Shani, M., Jansen, S., et al. 2002. Arteriolar and venular patterning in retinas of mice selectively expressing VEGF isoforms. *J. Clin. Invest.* 109:327-336.

7. Yaniv, K., Isogai, S., Castranova, D., Dye, L., Hitomi, J., and Weinstein, B.M. 2006. Live imaging of lymphatic development in the zebrafish. *Nat. Med.* 12:711-716.

A

MALDI-TOF-MS of 2-AB-labeled O-glycans of mouse endothelial cells and predicted compositions in positive mode

Composition	Observed *m/z*	Predicted *m/z*
$[Gal_1GalNAc_1\text{-}2AB\text{-}Na]^+$	526.6	526.4
$[GlcNAc_1\text{-}GalNAc_1\text{-}2AB\text{-}H]^+$	545.4	545.3
$[GlcNAc_1\text{-}GalNAc_1\text{-}2AB\text{-}Na]^+$	567.6	567.3
$[GalNAc_1\text{-}SA_1\text{-}H]^+$	632.6	632.5
$[Fuc_1Gal_1GalNAc_1\text{-}2AB\text{-}Na]^+$	672.2	672.5
$[GlcNAc_1Gal_1GalNAc_1\text{-}2AB\text{-}H]^+$	707.8	707.5
$[Fuc_1Hex_1Gal_1GalNAc_1\text{-}2AB\text{-}Na]^+$	812.5	812.6
$[Hex_3GalNAc_1\text{-}2AB\text{-}H]^+$	850.2	850.6
$[Gal_1GlcNAc_1Gal_1GalNAc_1\text{-}2AB\text{-}Na]^+$	891.3	891.7
$[Fuc_1Fuc_1Gal_1Gal_1GalNAc_1\text{-}2AB\text{-}Na]^+$	980.3	980.8

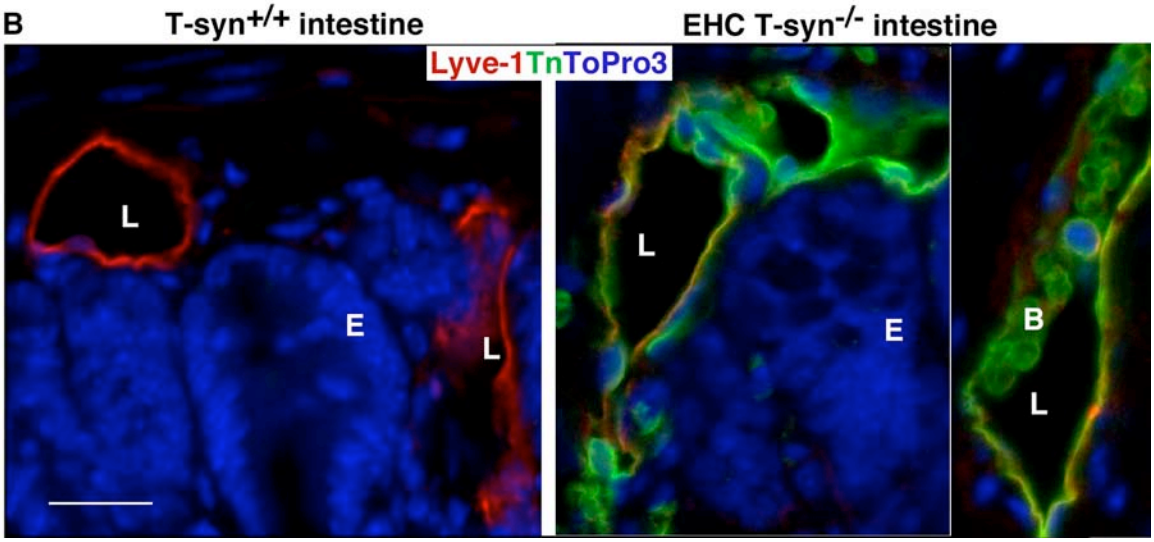

Supplemental Figure 1

(A). MADI-TOF-MS analysis of 2-AB-labeled O-glycans of mouse endothelial cells and predicted compositions in a linear positive mode. (**B**). Immunofluorescent staining of intestinal sections with antibodies to Tn antigen and Lyve-1. ToPro3 stains cell nuclei. L, lymphatic vessel; B, blood cells; E, epithelial cells. Scale bar: 20 μm.

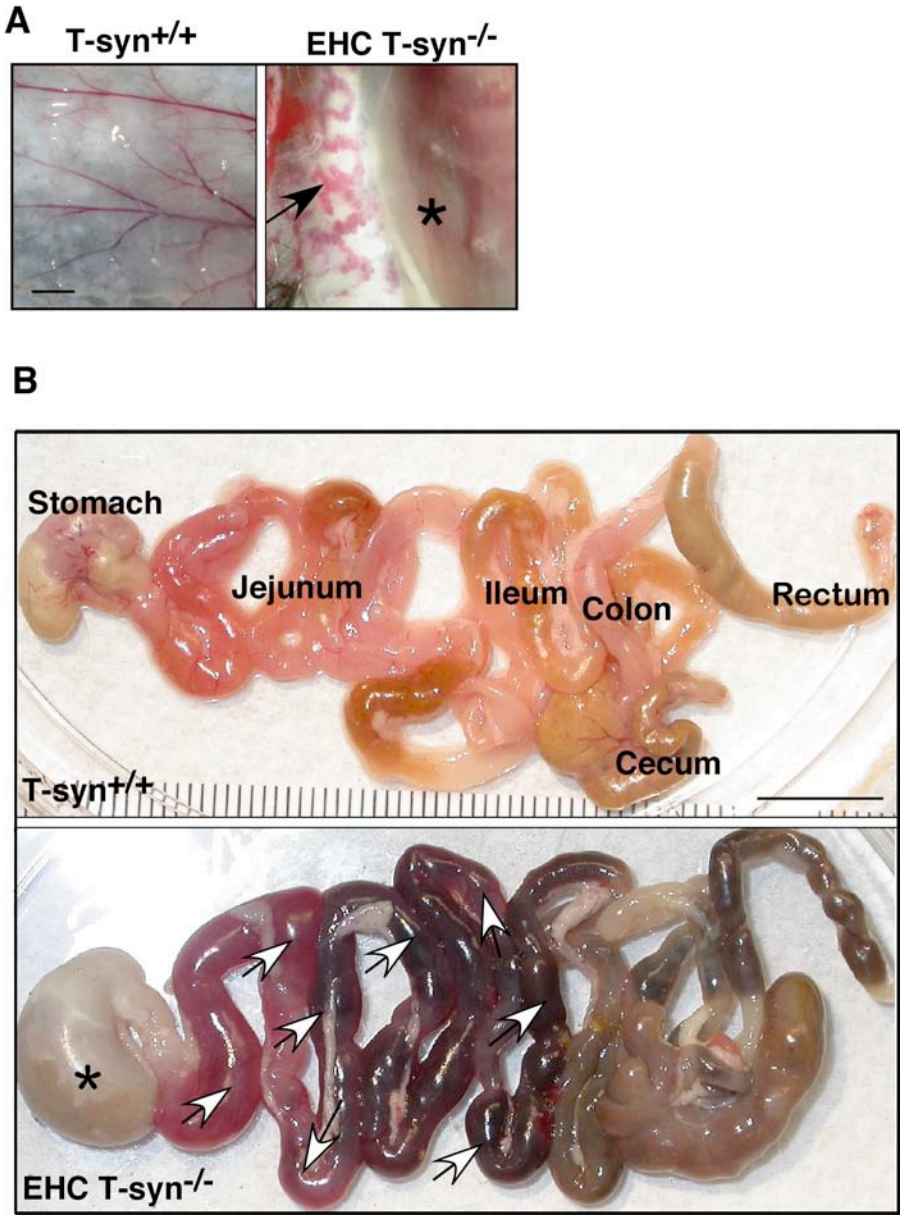

Supplemental Figure 2

EHC T-syn$^{-/-}$ mice also exhibit skin vascular abnormalities associated with subcutaneous edema and often have gastrointestinal bleeding. (**A)** Subcutaneous vasculature of 3-month-old T-syn$^{+/+}$ and EHC T-syn$^{-/-}$ mice. Arrow indicates vessels with blind ends. Asterisk marks edema. (**B**) T-syn$^{+/+}$ and EHC T-syn$^{-/-}$ gastrointestinal tracts. Arrows show widespread intestinal bleeding in the

EHC T-syn$^{-/-}$ tract; the EHC T-syn$^{-/-}$ stomach (asterisk) is highly dilated due to intestinal bleeding and/or obstruction. Mouse age: 3 weeks old. Scale bars: A, 1 mm; B, 1 cm.

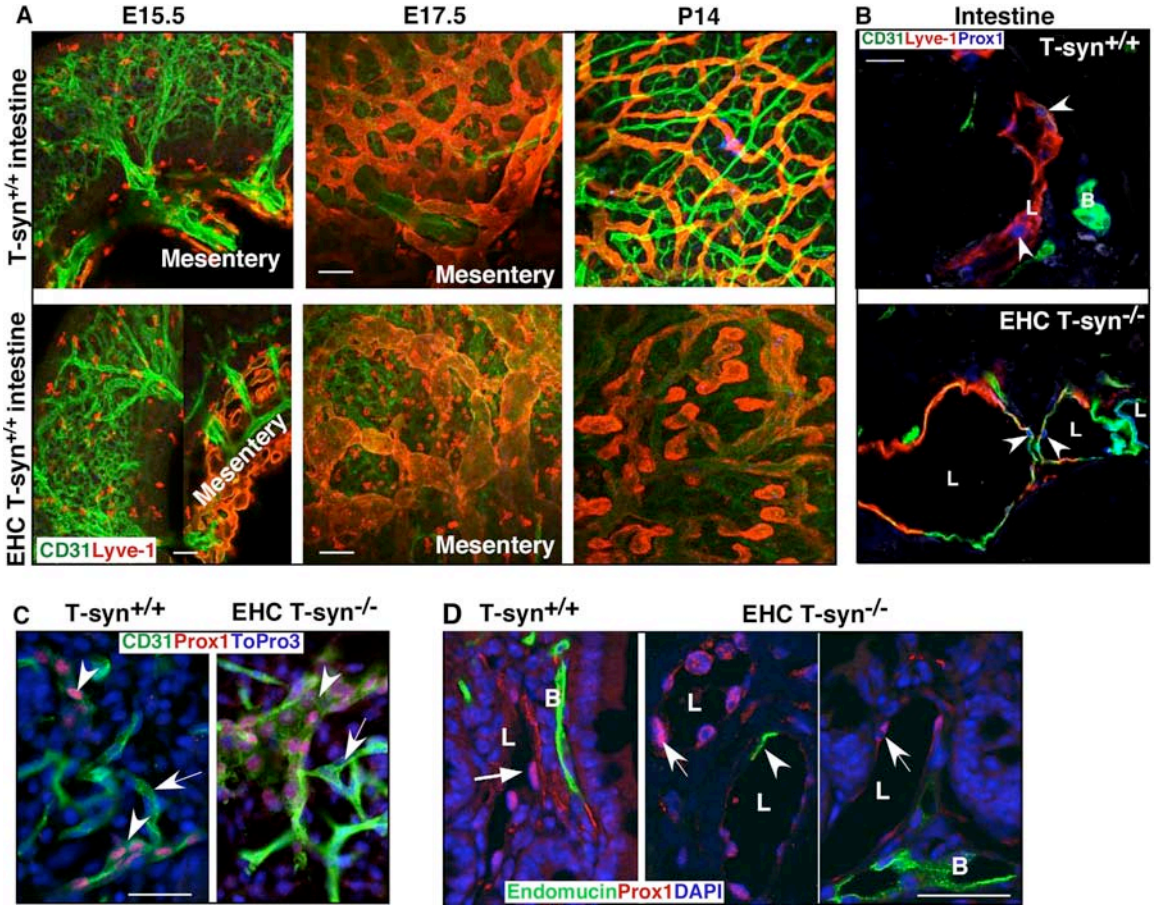

Supplemental Figure 3

EHC T-syn$^{-/-}$ lymphatic capillaries exhibit distorted shapes. (**A**) Confocal analysis of blood and lymphatic vessels of small intestines at different developmental stages. (**B**) Cryosections of intestines labeled with antibodies to CD31, Lyve-1 and Prox1. Arrowhead indicates Prox1 staining. (**C**) Skin microvascular network labeled with antibodies to CD31 and Prox1. ToPro3 is nuclear staining. Arrow indicates blood capillaries. Arrowhead indicates lymphatic vessels. (**D**) Intestinal microvessels labeled with antibodies to endomucin and Prox1. Arrow indicates Prox1 staining. Arrowhead marks ectopic endomucin staining in lymphatic

vessels. Scale bar: 50 μm. B, blood vessel; L, lymphatic vessel. 5-week-old intestinal tissues were analyzed in B, C, and D.

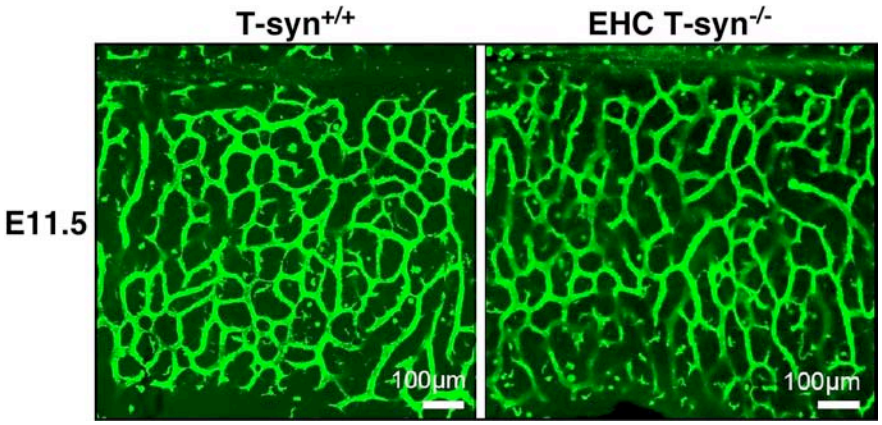

Supplemental Figure 4

EHC T-syn$^{-/-}$ mice do not have significant blood vascular abnormalities in brain. Confocal imaging of E11.5 T-syn$^{+/+}$ and EHC T-syn$^{-/-}$ vascular networks in the hindbrain.

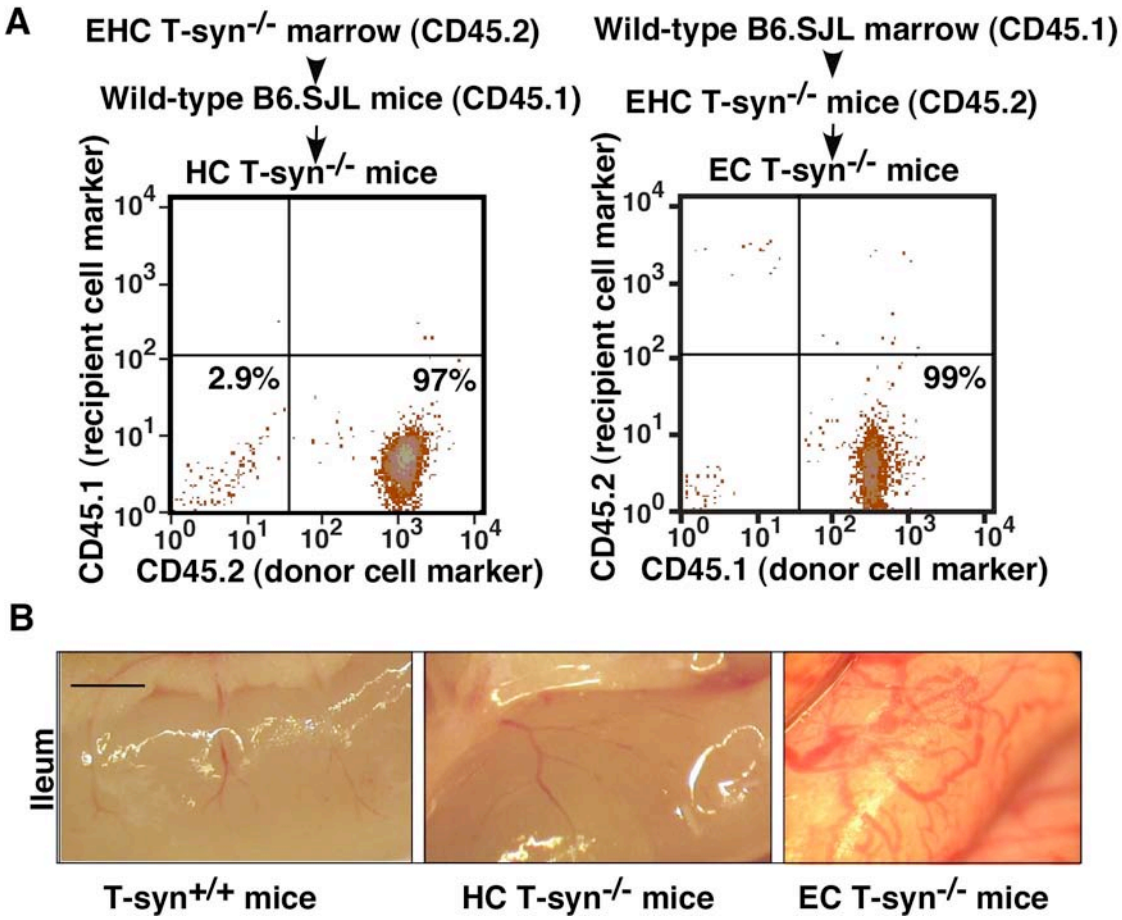

Supplemental Figure 5

(A) Generation of HC T-syn$^{-/-}$ and EC T-syn$^{-/-}$ mice by bone marrow transplantation. Representative flow cytometric data show donor cell engraftment in recipient bone marrows. (**B**) Intestinal vasculature of HC T-syn$^{-/-}$ and EC T-syn$^{-/-}$ mice at 9 months after bone marrow transplantation. n = 3. Scale bar: 1 mm.

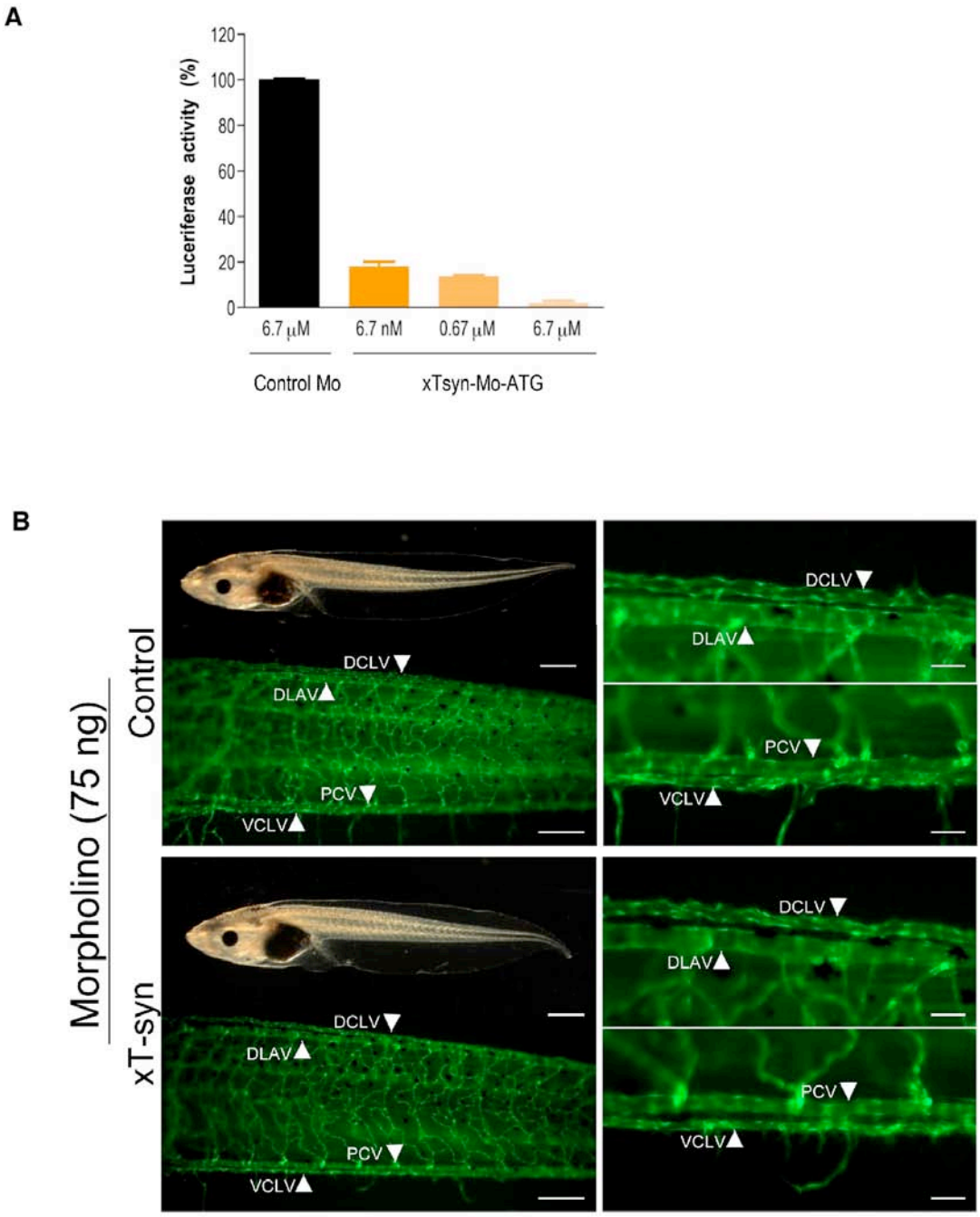

Supplemental Figure 6

Blood and lymphatic vessels develop normally in T-syn^{KD} *Xenopus laevis* embryos. (**A**) xTsyn-MO-ATG dose-dependently block translation of *Xenopus laevis* T-syn (xTsyn) (orange bars) as compared to control morpholino (black bar)

using the chimeric xTsyn/luciferase reporter assay. Error bars represent the SEM. (**B**) Left panel: Bright field images of stage 48 (8 dpf) tadpoles showing overall normal morphology and lack of hemorrhages in xT-syn^{KD} embryos. Fluorescent imaging revealing normal blood- and lymph vessel in trunk of xT-syn^{KD} embryos. Right panels: Higher magnifications of the same images as in the left panels. DCLV, dorsal caudal lymphatic vessel; DLAV, dorsal longitudinal anastomosing vessel; PCV, posterior cardinal vein; VCLV, ventral caudal lymph vessel. Scale bar represents 1 mm in left panels (bright field images); 200 μm in left panels (fluorescent images); 50 μm in right panels. In all panels, the tadpoles are oriented with their heads facing left.

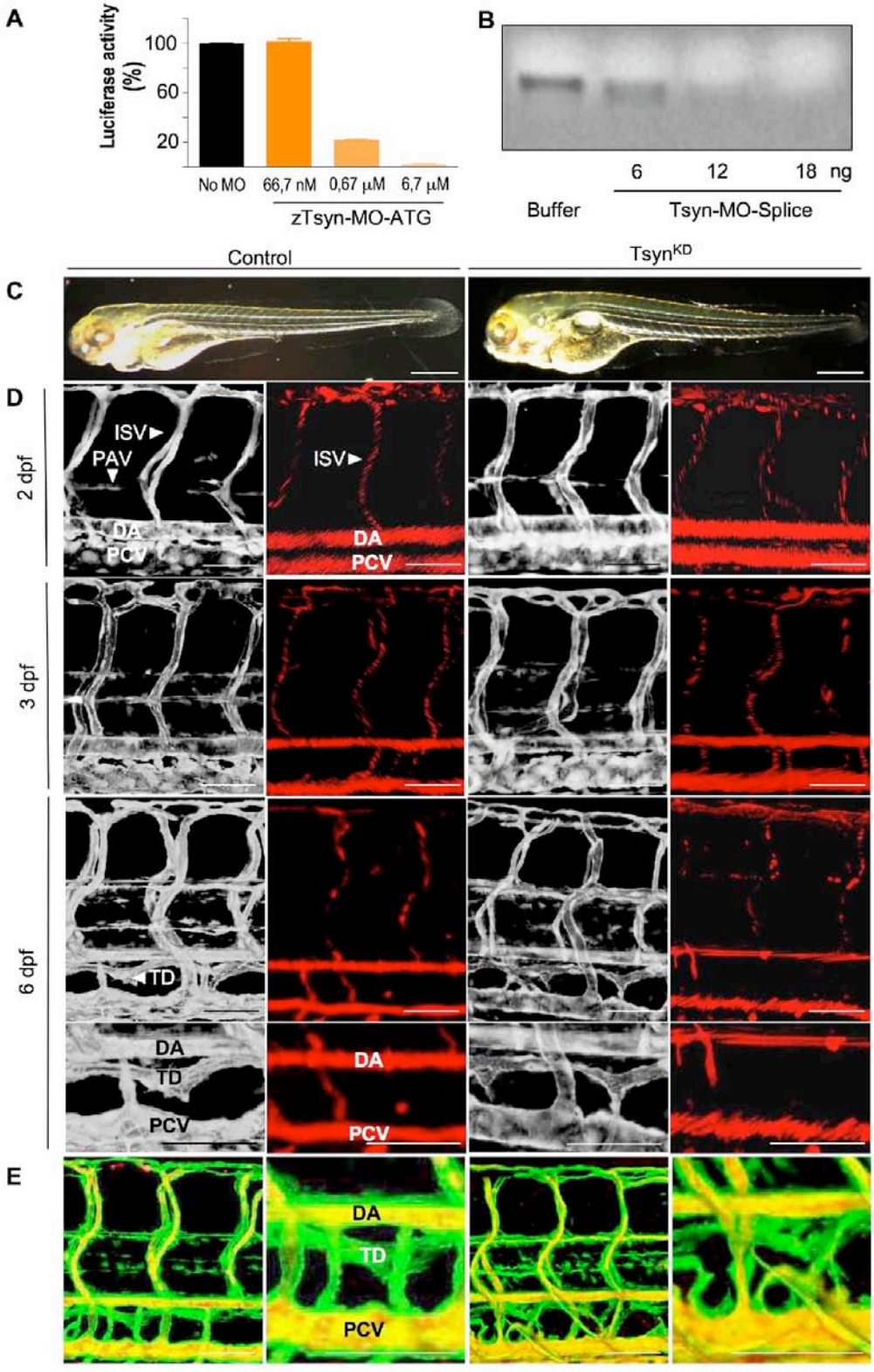

Supplemental Figure 7

Blood and lymph vessels develop normally in zTsyn^{KD} zebrafish embryos. (**A**) zTsyn-MO-ATG dose-dependently blocked translation of zebrafish T-syn (zTsyn) (orange bars) as compared to control sample without morpholino (black bar) using the chimeric zTsyn/luciferase reporter assay. Error bars represent the SEM. (**B**) RT-PCR analysis, revealing that zTsyn-MO-Splice dose-dependently decreased zTsyn transcript levels in 2 dpf zTsyn^{KD} embryos. (**C**) Bright field images showing overall normal morphology and lack of hemorrhages in 6 dpf zTsyn^{KD} embryos. (**D**) Left panels, confocal images of 2,3 and 6 dpf *Tg(fli1:EGFP)^{y1}* embryos showing normal development of the dorsal aorta (DA), posterior cardinal vein (PCV), intersomitic vessels (ISVs), parachordal vessel (PAV) as well as the thoracic duct (TD) in zTsyn^{KD} and control embryos. Right panels, confocal images of DsRed+ erythrocytes (red) in 2,3 and 6 dpf *Tg(gata-1:DsRed)* embryos revealing normal blood flow in the DA, PCV and ISVs but absence of red blood cells in the TD of zTsyn^{KD} embryos. Lower panels at 6 dpf represent magnifications of upper panels. (**E**) Angiography of 6 dpf *Tg(fli1:EGFP)^{y1}* embryos injected with dextran tetramethylrhodamin labeling the DA, PCV and ISVs (red/yellow), but not the TD (green) in control and zTsyn^{KD} embryos. Right panels are higher magnifications. (**C - E**) Head faces to the left in all panels. Scale bar represents 200 μm in (**C**) 40 μm in (**D, E**).

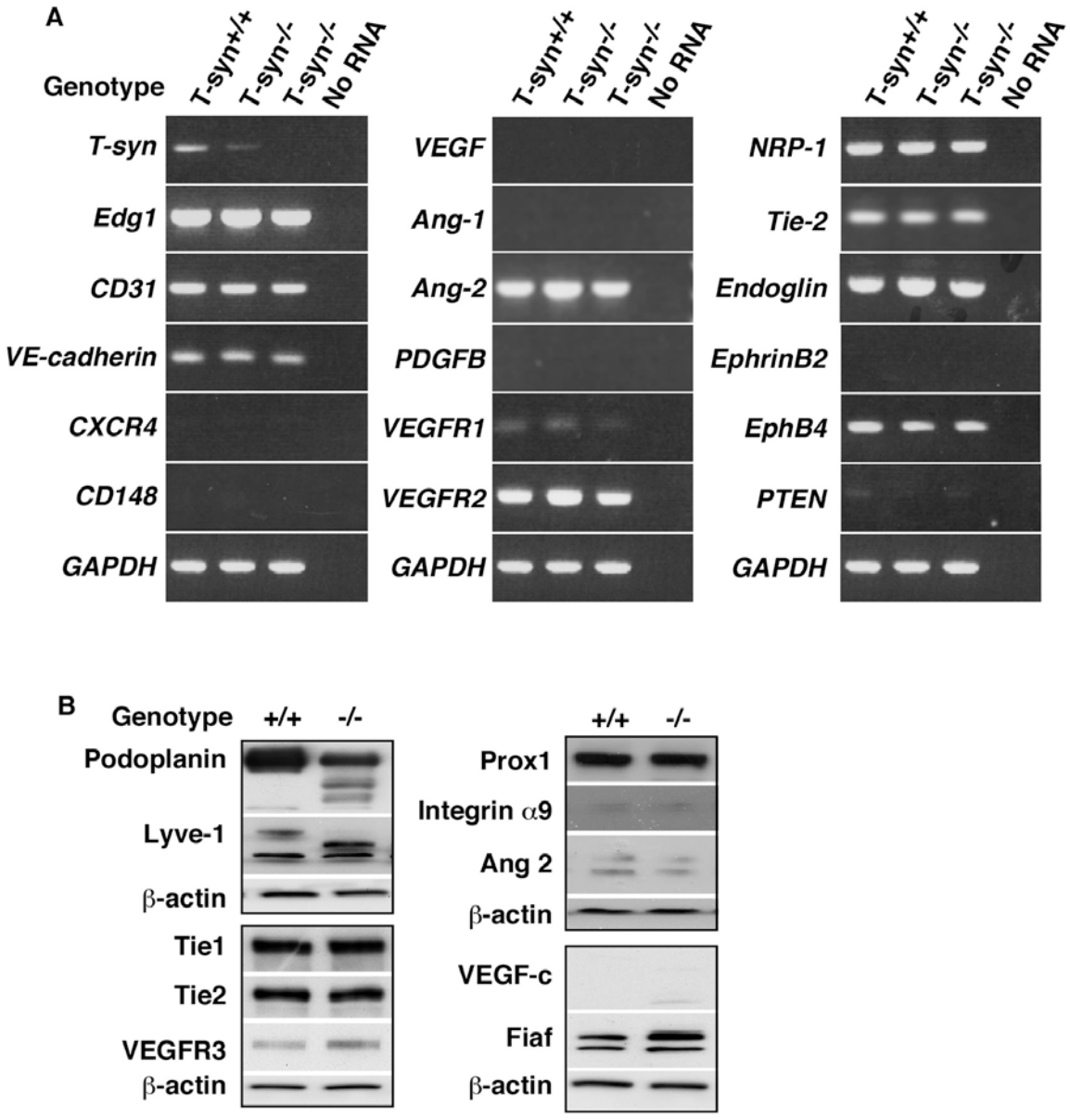

Supplement Figure 8

Expression profiles of mRNAs and protein levels of candidate O-glycoproteins. (**A**) Semi-quantitative RT-PCR profile of endothelial cell genes that are related to angiogenesis and lymphangiogenesis. The housekeeping gene *GAPDH* was used as a loading control. (**B**) Protein expression in primary endothelial cells measured by western blotting with antibodies to glycoproteins that are involved in

vascular development. β-actin was used as a loading control. Small intestine lysates were used to analyze VEGF-C and Fiaf. Data are representative of three independent experiments.

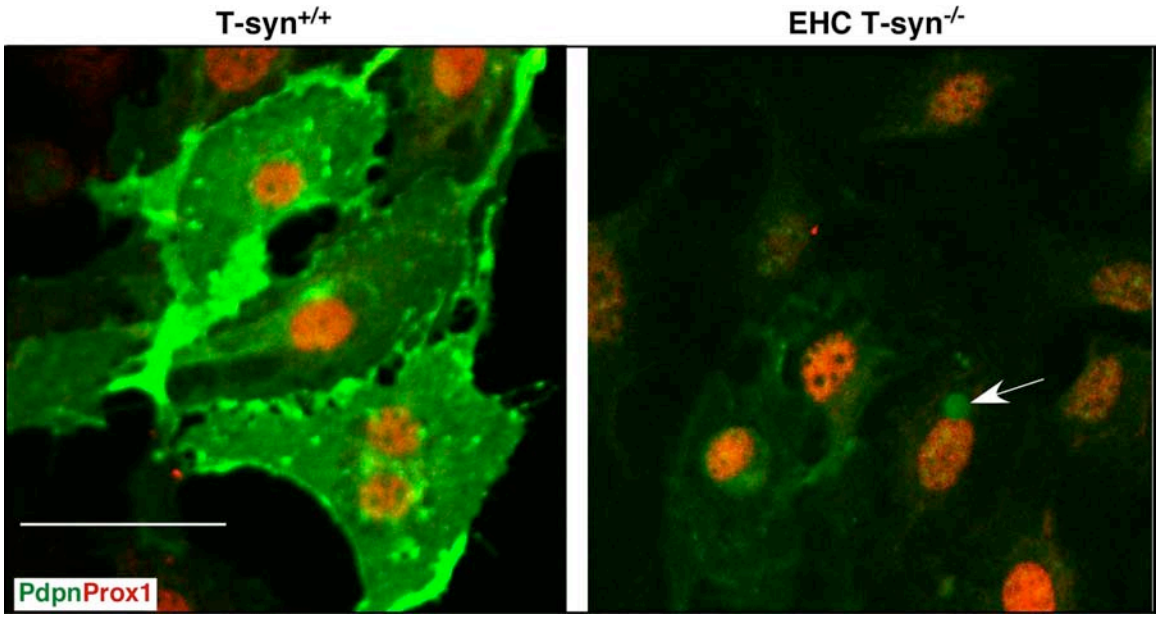

Supplemental Figure 9

The expression of surface podoplanin is significantly impaired in Prox1-positive primary skin lymphatic endothelial cells from EHC T-syn$^{-/-}$ mice. Immunofluorescent staining of permeabalized lymphatic endothelial cells. Arrow indicates autofluorescence of a magnetic bead used for cell sorting. Scale bar: 50 μm.

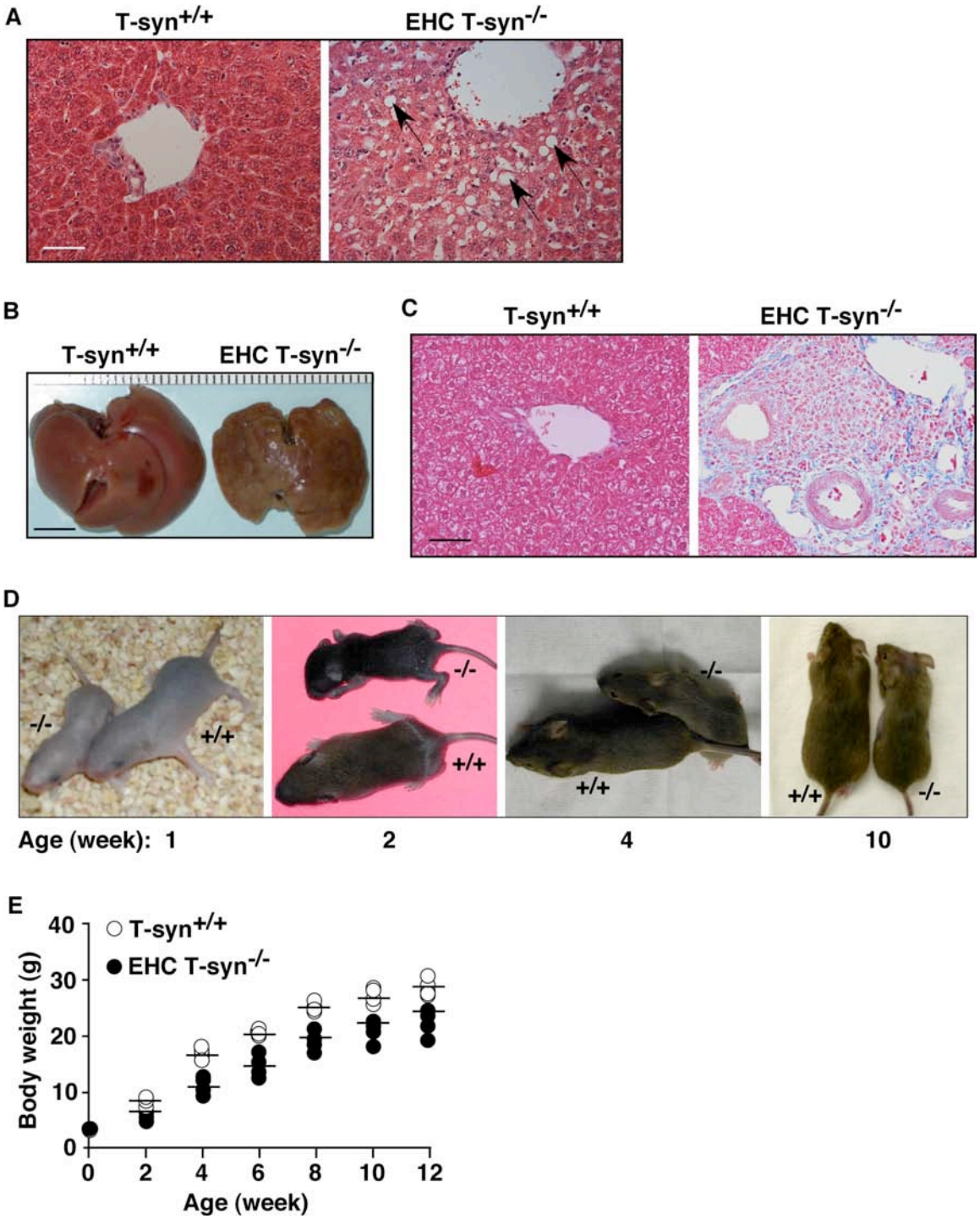

Supplemental Figure 10

EHC T-syn$^{-/-}$ mice develop fatty liver disease. **(A)** Histological analysis of P7 livers (H&E). Arrows indicate macrovesicular steatosis. **(B)** Gross morphology of

livers from 3-month-old T-syn$^{+/+}$ and EHC T-syn$^{-/-}$ mice. EHC T-syn$^{-/-}$ liver is shrunken and cirrhotic with nodular and yellowish-tan appearance. (**C**) Masson's trichrome staining shows perivenular fibrosis in EHC T-syn$^{-/-}$ liver (blue staining). **(D** and **E)** EHC T-syn$^{-/-}$ mice had lower body weight at different developmental stages than the controls. (**F**) Abnormal lipid deposition is revealed by Nile red staining (red) in livers of 9-month-old WT and inducible T-syn$^{-/-}$ mice. Scale bars: A and C, 100 μm; B, 5 mm.

Supplemental videos

Intravital microscopic videos reveal abnormal connections between veins and lymphatic vessels in inducible T-syn$^{-/-}$ mice. Videos clips of T-syn$^{+/+}$ (**1**) and inducible T-syn$^{-/-}$ (**2**) intestinal vessels before and after an arterial injection with India ink.